

# Rapidity Spectra of the Secondaries Produced in Heavy Ion Collisions and the Constituent Picture of the Particles

Bhaskar De\*

*Institute of Mathematical Sciences,*

*C.I.T. campus, Taramani,*

*Chennai-600113, India*

S. Bhattacharyya<sup>†‡</sup>

*Physics and Applied Mathematics Unit(PAMU),*

*Indian Statistical Institute, Kolkata - 700108, India*

(Dated: January 27, 2020)

## Abstract

The present study is both a reanalysis and an extension of the approach initiated by Eremin and Voloshin(referenced in the text). We attempt to interpret here the rapidity-spectra of the various particles produced in both  $Pb + Pb$  and  $Au + Au$  collisions at CERN-SPS and RHIC-BNL. The study made here is wider in scope and is more species-specific than the earlier ones for which the results obtained here have been compared with those suggested by some previous works based on HIJING, VENUS etc, at various centralities. The study reconfirms that the constituent parton picture of the particles provides a better and more unified description of the rapidity-density yields for the various secondaries, including some light cluster particles like deuteron even in heavy ion collisions.

PACS numbers: 25.75.-q

Keywords: Relativistic Heavy Ion Collision

---

<sup>†</sup> Communicating Author

\*Electronic address: bhaskar@imsc.res.in

<sup>‡</sup>Electronic address: bsubrata@isical.ac.in

## I. INTRODUCTION

In the recent past Eremin and Voloshin[1] proposed that both nucleons and individual nuclei could be considered as superposition of the constituents (of the particles) called partons/quarks/valons etc. Normally it is assumed that the nucleons are built of three such constituent partons and the mesons are composed of two of them. Such a constituent picture helps us to interpret the deep inelastic collision processes involving lepton-hadron, hadron-hadron and hadron-nucleus collisions. Much earlier, Bialas et al studied to explore the hypothesis, within the framework of the additive quark model(AQM)[2], that the constituent partons(quarks) provide the universal elements not only of nucleon-nucleon and nucleon-nucleus reactions but also nucleus- nucleus interactions at high energies; this study ended up with surely an affirmative indication to such a possibility. But, as the focus was on different issues, the central theme of this work deviated from what it is intended to be here. We will simply look into the behaviour of some chosen observables studied here for nucleus-nucleus collisions alone from the viewpoint of such partonic constituent pictures. The centrality-dependence of multiplicity-density offers a very fundamental observable and we present here our studies on production of pions, kaons, protons and antiprotons separately in both  $Pb + Pb$  (including deuteron production for this collision) at CERN-SPS and  $Au + Au$  collisions at RHIC-BNL at  $\sqrt{s_{NN}} = 130$  and 200 GeV respectively. Besides, very recently the data on deuteron production in  $Pb + Pb$  collision have been obtained, for which they have also been taken here into account. This apart, we will also compare the performance of the present approach with those obtained on the basis of some standard-version programmings like HIJING, VENUS etc which are essentially much more complicated than the one dealt with here. Our objective here is to examine the efficacy of this approach in explaining some relevant data on production of these very important kind of secondaries in the few now available high energy nuclear collisions. The approach was also successfully tested for production of neutral particles, like photons, by Netrakanti and Mohanty[3] in the very recent past and was found to be in accord with the contention of Eremin and Voloshin[1].

## II. THE OUTLINE OF THE CALCULATION OF THE NUMBER OF PARTICIPANTS

In course of our calculations for the number of participant nucleons, denoted by  $N_{n-part}$ , and the number of participant partons, denoted by  $N_{q-part}$  we follow exactly the ways adopted by Eremin and Voloshin[1] and Netrakanti and Mohanty[3], wherein a Woods-Saxon nuclear density profile is taken into account. This is given by

$$n_A(r) = \frac{n_0}{1 + \exp [(r - R)/d]} \quad (1)$$

where  $n_0 = 0.17 \text{ fm}^{-3}$ ,  $R = (1.12A^{1/3} - 0.86A^{-1/3}) \text{ fm}$ ,  $d = 0.54 \text{ fm}$ .

The number of participant nucleons( $N_{n-part}$ ) for a nucleus-nucleus( $A + B$ ) collision at an impact parameter  $b$  is calculated using the expression[1, 3],

$$\begin{aligned} N_{n-part}|_{AB} &= \int d^2s T_A(\vec{s}) \{1 - [1 - \frac{\sigma_{NN}^{inel} T_B(\vec{s}-\vec{b})}{B}]^B\} \\ &+ \int d^2s T_B(\vec{s}-\vec{b}) \{1 - [1 - \frac{\sigma_{NN}^{inel} T_A(\vec{s})}{A}]^A\}, \end{aligned} \quad (2)$$

where  $A$  and  $B$  are the mass numbers of the two colliding nuclei,  $T(b) = \int_{-\infty}^{\infty} dz n_A(\sqrt{b^2 + z^2})$  is the thickness function, and  $\sigma_{NN}^{inel}$  is the inelastic nucleon-nucleon cross section. The number of participant partons is also calculated in a similar manner by taking into account the following changes of the facts related to physical realities, viz., (i) the density is changed to three times that of nucleon density with  $n_0^q = 3n_0 = 0.51 \text{ fm}^{-3}$ ; (ii) the cross sections are changed to  $\sigma_{qq} = \sigma_{NN}^{inel}/9$  and (iii) the mass numbers of the colliding nuclei are changed to three times of their values keeping the size of the nuclei same as in the cases of  $N_{n-part}$ [1, 3].

In the same way, the number of participant partons in a  $PP$  or  $P\bar{P}$  collision can also be calculated by using  $A = 3$  and  $B = 3$ , and considering nucleons as hard spheres of uniform radii  $0.8 \text{ fm}$ [4].

For the present work we use  $\sigma_{NN}^{inel} = 30 \text{ mb}$  in the range of c.m. energies  $\sqrt{s_{NN}} = 4-17.3 \text{ GeV}$  as suggested in Ref.[5]. For higher energies, we first fit the data on total cross-sections for  $PP$  and  $P\bar{P}$  collisions[6] at energies beyond  $\sqrt{s_{NN}} = 30 \text{ GeV}$  with the expression[7]

$$\sigma_{NN}^{total} = (29.2 \pm 0.3) [1 + \frac{(2.2 \pm 0.5) \text{ GeV}}{\sqrt{s_{NN}}}] + (1.1 \pm 0.1) \ln(\frac{s_{NN}}{10 \text{ GeV}^2}) + (0.19 \pm 0.01) \ln^2(\frac{s_{NN}}{10 \text{ GeV}^2}) \quad (3)$$

with  $\chi^2/ndf = 171/47$ , where  $ndf = \text{No. of data} - \text{No. of Parameters}$ . We also fit the elastic cross-section data for the same interactions[6] with a similar type of expression which is given by,

$$\sigma_{NN}^{elastic} = (6.2 \pm 0.2) \left[ 1 + \frac{(4.8 \pm 1.4) \text{ GeV}}{\sqrt{s_{NN}}} \right] - (0.47 \pm 0.04) \ln \left( \frac{s_{NN}}{10 \text{ GeV}^2} \right) + (0.11 \pm 0.01) \ln^2 \left( \frac{s_{NN}}{10 \text{ GeV}^2} \right) \quad (4)$$

with  $\chi^2/ndf = 53.14/18$ . The fits along with the data are shown in Fig.1. Hence, one can obtain the energy-dependence of inelastic cross-section ( $\sigma_{NN}^{inel}$ ) for nucleon-nucleon interaction by subtracting eqn.(4) from eqn.(3). The values of  $\sigma_{NN}^{inel}$ , obtained in this manner, at some energies are given in Table-I. The obtained values fall within 6% error of those suggested in Ref.[5]. But a point is to be noted. Though some sort of justification for proposing the nature of the total cross section in the form of expression (3) given in Ref.[7], none such explanation for expression (4) is possible. This is simply assumed with a view to providing only a best fit to the available data on elastic cross section shown in Fig.1 and extracting a workable phenomenological form of expression for the nature of inelastic cross section,  $\sigma_{NN}^{inel}$ . In fact, these twin relations help us to arrive at the usable values of inelastic cross sections needed for our necessary calculations of the relevant observables in a systematic manner even at energies for which no measured data on cross section values are available.

### III. RESULTS AND DISCUSSIONS

The values of the number of participant nucleons and those of the participant partons for three nucleus-nucleus collisions at various energies and different centralities are presented in the Tables(II- IV). A comparison of the results obtained on the basis of the present work with those of NA49[8], WA98[9] and PHENIX[10, 11, 12] groups is made in Fig.-2(a) to Fig.-2(d), in terms of  $1 - \frac{\langle N_{n-part}^{PresentWork} \rangle}{\langle N_{n-part}^{NA49/WA98/PHENIX} \rangle}$  versus  $N_{n-part}^{NA49/WA98/PHENIX}$ . It is observed that the agreements in cases of Au+Au collisions are modestly fair, whereas for Pb+Pb interaction the disagreement is quite strong and prominent. This discrepancy could, for the present, be attributed to the much less c.m energy in lead-lead reaction which falls roughly at 17.2 GeV only.

The integrated yields of the identified hadrons at central rapidity region produced in  $Pb + Pb$  and  $Au + Au$  collisions at different centralities are presented diagrammatically in

Fig.3-Fig.5. In subfigures labelled as (a) and (b) of each category, the experimental data on integrated yields are normalized by half of the number of participant nucleons( $N_{n-part}$ ) while those in subfigures labelled as (c) and (d) are normalized by half of the number of participant partons( $N_{q-part}$ ). As we are here to make comparison between these two cases, we should use values of both the observables obtained from a single model. And that is why we put into use the values of  $\langle N_{n-part} \rangle$  obtained on the basis of the present work, instead of the values indicated by NA49[8] or PHENIX groups[10, 11, 12].

Now, to make a comparison between these two cases we fit the data in Fig.3-Fig.5 by two phenomenological expressions which are given by,

$$\frac{1}{0.5 \langle N_{n-part} \rangle} \frac{dN_{ch}}{dy} = a N_{n-part}^{\alpha} \quad (5)$$

and

$$\frac{1}{0.5 \langle N_{q-part} \rangle} \frac{dN_{ch}}{dy} = b N_{q-part}^{\beta} \quad (6)$$

where  $a$ ,  $b$ ,  $\alpha$  and  $\beta$  are four constants. The fitted values of these parameters are given in Tables(V-VII) and depicted by solid curves in the figures. As could be seen from Fig.2 that the most peripheral values of  $N_{n-part}$  for  $Pb+Pb$  collision at  $E_{Lab} = 158A$  GeV and  $Au+Au$  collision at  $\sqrt{s_{NN}} = 200$  GeV obtained by the present model show larger discrepancies with respect to those obtained by NA49 and PHENIX collaborations, we keep most peripheral data in these two collisions out of the range of both the fits provided by eqn.(5) and eqn.(6).

Obviously, the factors  $\alpha$  and  $\beta$  provide the slopes of the fits. As the magnitude of any of these factors takes value nearer to zero, the fit will exhibit better flatness of the data with respect to  $N_{n-part}$  or  $N_{q-part}$  implying a superior compliance of scaling, i.e., a better scaling. A look at Table-V reveals that the data on  $\langle \pi \rangle$ ,  $K^{\pm}$  and  $P/\bar{P}$  in  $Pb+Pb$  collisions show a better degree of conformity with scaling when normalized by half of  $N_{q-part}$ , as in all cases  $|\beta|$  is less than  $|\alpha|$ . But, for the case of deuteron production in  $Pb+Pb$  collision, the scenario is just the opposite. Besides, the integrated yields for charged pions produced in  $Au+Au$  interactions at both the RHIC energies[Tables VI - VII] do not exhibit scaling satisfactorily, when the data are normalized by half of  $N_{q-part}$  instead of  $N_{n-part}$ , as the values of  $|\alpha|$ , in these cases, are quite small with respect to  $|\beta|$ . However, the data on  $K^{\pm}$  and  $P/\bar{P}$  produced in the same collisions favour the  $N_{q-part}$ -scaling over the  $N_{n-part}$ -scaling, though the cases

of  $P/\bar{P}$  at  $\sqrt{s_{NN}} = 200$  GeV are not as prominent as in the other cases. In fine, our net finding from the present study is the pions do not agree, while the kaons and protons do.

The Fig.6(a) deserves some special attention and comments. The plots on integrated yields for charged hadrons produced in both nucleus-nucleus( $A + A$ ) and  $P + \bar{P}$  collision deflect from each other when data on both are separately normalized in terms of number of participating nucleons( $N_{n-part}$ ). The data on integrated yields in central nucleus-nucleus collisions normalized by the number of participant nucleon-pair have been used here from Fig.3 of Ref.[13]. To our purpose, this has to be normalized in terms of the basic parton(quark)-constituents, denoted by  $\langle N_{q-part} \rangle$ , for which the (charged)pseudo-rapidity density terms for various nucleus-nucleus collisions normalized by participant nucleon-pair, i.e., the factors  $\frac{1}{0.5\langle N_{n-part} \rangle} \frac{dN_{ch}}{d\eta}$  are to be multiplied by  $R = \langle N_{n-part} \rangle / \langle N_{q-part} \rangle$  with the values of them as given in Table-VIII. And, in this conversion we have utilized those particular values of  $\langle N_{n-part} \rangle$  as were used in Ref.[13], so that we can normalize the exact values of  $\frac{dN_{ch}}{d\eta}$  by  $\langle N_{q-part} \rangle / 2$ . In calculating  $N_{q-part}$  for  $P + \bar{P}$  collisions, we use equation(2) and the values of  $N_{q-part}$  for  $P + \bar{P}$  collisions at three different c.m. energies are given in Table-IX as a function of relative probability.

And when partonic considerations are used in normalization, the data on both  $P + \bar{P}$  and  $A + A$  collisions come to an agreeable state. The  $\langle N_{q-part} \rangle$ -values that are to be used for normalization of the most central  $P + \bar{P}$  collisions, i.e., 0 – 5% central collisions are depicted in Table-X. In order to check the nature of agreement between the data on  $A + A$  and  $P + \bar{P}$  collisions, we try to obtain a fit by taking into account both sets of data, normalized by  $\langle N_{q-part} \rangle / 2$ ; and the desired fit is to be described here by the following expression:

$$\frac{1}{0.5 \langle N_{q-part} \rangle} \frac{dN_{ch}}{d\eta} = - (0.010 \pm 0.003) + (0.27 \pm 0.01) \ln \left( \frac{\sqrt{s_{NN}}}{GeV} \right) \quad (7)$$

with  $\chi^2/ndf = 3.632/12$ . The goodness of the fit is also shown in Fig.6(b) with the help of the expression  $fit - data$  as a function of  $\sqrt{s_{NN}}$  which reveals that both sets of data are in good agreement with respect to the fit. Hence, both  $A + A$  and  $P + \bar{P}$  data exhibit a common  $\sqrt{s_{NN}}$ -dependence when the data on the former are normalized by the number of participant parton-pairs.

#### IV. CONCLUDING REMARKS

Let us now summarize our observations made here: (i) The secondaries, excluding deuterons, produced in  $Pb + Pb$  collision at CERN-SPS behave modestly well vis-a-vis  $N_{q-part}$  scaling. The behaviour is more consistent towards the highest values of centrality, with centrality maximum at 0-5% (represented by solid boxes in the graph). (ii) Similar statements could be made about  $Au + Au$  interactions at both energies (Fig.4 and Fig.5) except the cases for pions. (iii) It is quite noticeable that there are modest degree of divergences in the  $N_{n-part}$ -values between the calculations done by us at different centralities and those by others, as indicated in the text (in the second and third columns of the various Tables presented in this work). For the present, these discrepancies could be attributed only to our much simpler programming than what is resorted to by the big groups like NA49, WA98, PHENIX etc. The plain fact is we are now simply unable to take up such rigorous studies as might be desired or advisable due to various reasons beyond our capacity and control. But, we recognize the urgency and importance of such studies in order to arrive at a decision about the merit of  $N_{q-part}$  scaling and of the viewpoints expressed by Eremin and Voloshin[1]. (iv) The Fig.6 highlights on how the data on both  $P + \bar{P}$  and  $A + A$  collisions negotiate better the idea of partonic-participant scaling, when the constituent-participant number for both  $P + \bar{P}$  and  $A + A$  collisions are taken into account. Thus, the present study does essentially provide modest support to the viewpoints expressed by Eremin and Voloshin in their work of Ref.[1].

#### Acknowledgments

The authors are very grateful to the anonymous referee for his/her very patient readings, constructive criticisms and kind valuable instructions for the improvements in the previous drafts of the manuscript. The authors would also like to express their thankful gratitude to Professor D. Miśkowiec for providing some helpful suggestions about running the FORTRAN code developed by him in calculating the number of participants,  $N_{part}$ . One of the authors, BD, is thankful to the IMSc for offering him the support by a post-doctoral Fellowship of the IMSc, wherein a part of this work was done.

- 
- [1] S. Eremín and S. Voloshin: Phys. Rev. **C 67**(2003) 064905.
- [2] A. Bialas, W. Czyz and L. Lesniak: Phys. Rev. **D 25**(1982)2328.
- [3] P. K. Netrakanti and B. Mohanty: Phys. Rev. **C 70**(2004) 027901; nucl-ex/0401036.
- [4] C. Y. Wong: Introduction to High-Energy Heavy Ion Collisions, pg.161, World Scientific, 1994.
- [5] D. Miškowicz: <http://www-linux.gsi.de/~misko/overlap/manual.ps>.
- [6] Particle Data Group: <http://pdg.lbl.gov/2004/hadronic-xsections/hadron.html>
- [7] B. De, S. Bhattacharyya and P. Guptaroy: Jour. Phys. **G 27**(2001)2389.
- [8] J. Bachler et al(NA49 Collaboration): Nucl. Phys. **A 661**(1999)45c.
- [9] M. M. Aggarwal et al(WA98 Collaboration): Eur. Phys. Jour. **C 23**(2002)225.
- [10] K. Adcox et al(PHENIX Collaboration): Phys. Rev. **C 69**(2004)024904.
- [11] K. Adcox et al(PHENIX Collaboration): Phys. Rev. Lett. **86**(2001)3500.
- [12] S. Adler et al(PHENIX Collaboration): Phys. Rev. **C 69**(2004)034909.
- [13] B. B. Back et al(PHOBOS Collaboration): Phys. Rev. Lett. **88**(2002) 022302 and the references therein.
- [14] J. Klay: Ph. D. Thesis, University of California, Davis Dissertation, 2001, pg.127; [http://nuclear.ucdavis.edu/~jklay/CV/JLK\\_cv.html](http://nuclear.ucdavis.edu/~jklay/CV/JLK_cv.html).
- [15] S. V. Afanasiev et al(NA49 Collaboration): Phys. Rev. **C 66**(2002)054902.
- [16] B. B. Back et al(PHOBOS Collaboration): Phys. Rev. Lett. **85**(2000) 3100.
- [17] T. Anticic et al(NA49 Collaboration): Phys. Rev. **C 69**(2004)024902.



TABLE I: Values of inelastic nucleon-nucleon cross-section at different energies. The second column provides the values obtained by subtracting eqn.(4) from eqn.(3). The last column gives the values as cited in Ref.[5].

$\sqrt{s_{NN}}(GeV)$	$\sigma_{NN}^{inel}(mb)$ (Present Work)	$\sigma_{NN}^{inel}(mb)$ (From Ref.[5])
53	35	-
56	35	37
130	40	41
200	42	42
540	48	-
630	49	-
900	51	-
1800	56	-

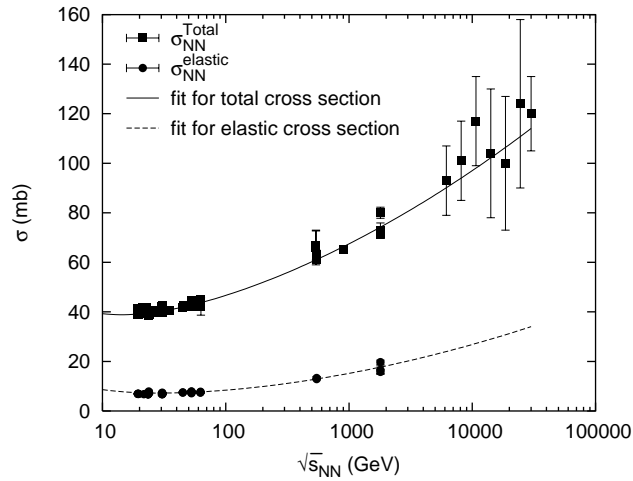


FIG. 1: Plots of total and elastic cross-section of  $PP$  and  $P\bar{P}$  interactions as a function of c.m. energies. Data points are taken from Ref.[6]. The solid curve depicts the fit for total cross-sections on the basis of eqn.(3) while the dashed one is for elastic cross-section on the basis of eqn.(4).

TABLE II: Values of  $\langle N_{n-part} \rangle$  and  $\langle N_{q-part} \rangle$  for  $Pb + Pb$  collisions at  $E_{Lab} = 158A$  GeV.

Centrality	$\langle N_{n-part}^{NA49} \rangle [8]$	$\langle N_{n-part}^{PresentWork} \rangle$	$\langle N_{q-part}^{PresentWork} \rangle$
0 – 5%	362	368	856
5 – 14%	305	290	644
14 – 23%	242	210	446
23 – 32%	189	140	278
32 – 47%	130	92	171
47 – 99%	72	32	53
Centrality	$\langle N_{n-part}^{WA98} \rangle [9]$	$\langle N_{n-part}^{PresentWork} \rangle$	$\langle N_{q-part}^{PresentWork} \rangle$
0 – 1%	$380 \pm 1$	385	901
1 – 6.8%	$346 \pm 1$	338	770
6.8 – 13%	$290 \pm 2$	273	600
13 – 25.3%	$224 \pm 1$	196	411
25.3 – 48.8%	$132 \pm 3$	99	189
48.8 – 67%	$63 \pm 2$	35	56
67 – 82.8%	$30 \pm 2$	10	14
82.8 – 100%	$12 \pm 2$	3	4

TABLE III: Values of  $\langle N_{n-part} \rangle$  and  $\langle N_{q-part} \rangle$  for  $Au + Au$  collisions at  $\sqrt{s_{NN}} = 130$  GeV.

Centrality	$\langle N_{n-part}^{PHENIX} \rangle$ [10, 11]	$\langle N_{n-part}^{PresentWork} \rangle$	$\langle N_{q-part}^{PresentWork} \rangle$
0 – 5%	$347.7 \pm 10$	351	880
5 – 10%	$293 \pm 10$	297	710.6
5 – 15%	$271.3 \pm 8.4$	272	645
10 – 15%	$248 \pm 8$	242.5	565.4
15 – 20%	$211 \pm 7$	207	469.4
20 – 25%	$177 \pm 7$	173	381
15 – 30%	$180.2 \pm 6.6$	174.5	387.3
25 – 30%	$146 \pm 6$	139	298
30 – 35%	$122 \pm 5$	120	249
35 – 40%	$99 \pm 5$	96	192
40 – 45%	$82 \pm 5$	81.5	158.7
45 – 50%	$68 \pm 4$	62	114.6
30 – 60%	$78.5 \pm 4.6$	77	150.1
60 – 92%	$14.3 \pm 3.3$	11.8	17.8

TABLE IV: Values of  $\langle N_{n-part} \rangle$  and  $\langle N_{q-part} \rangle$  for  $Au + Au$  collisions at  $\sqrt{s_{NN}} = 200$  GeV.

Centrality	$\langle N_{n-part}^{PHENIX} \rangle$ [12]	$\langle N_{n-part}^{PresentWork} \rangle$	$\langle N_{q-part}^{PresentWork} \rangle$
0 – 5%	$351.4 \pm 2.9$	351.9	880.1
0 – 10%	$325.2 \pm 3.3$	332.5	819.7
5 – 10%	$299.0 \pm 3.8$	292.2	694.6
10 – 15%	$253.9 \pm 4.3$	242.4	560.9
10 – 20%	$234.6 \pm 4.7$	226.2	517.4
15 – 20%	$215.3 \pm 5.3$	208.2	469
20 – 30%	$166.6 \pm 5.4$	157	339
30 – 40%	$114.2 \pm 4.4$	108.4	218
40 – 50%	$74.4 \pm 3.8$	71.5	134.3
50 – 60%	$45.5 \pm 3.3$	40.4	68.8
60 – 70%	$25.7 \pm 3.8$	23	35.6
60 – 80%	$19.5 \pm 3.3$	16.6	25
60 – 92%	$14.5 \pm 2.5$	11.8	17.3
70 – 80%	$13.4 \pm 3.0$	9.9	13.6
70 – 92%	$9.5 \pm 1.9$	6.8	9.1
80 – 92%	$6.3 \pm 1.2$	3.9	5

TABLE V: Values of  $a$ ,  $b$ ,  $\alpha$  and  $\beta$  for production of various secondaries in  $Pb + Pb$  collisions at  $E_{Lab} = 158A$  GeV[ndf=No. of data - No. of parameters in the fit].

Identified Secondary	$a$	$\alpha$	$\chi^2/ndf$	$b$	$\beta$	$\chi^2/ndf$
$\langle \pi \rangle$	$0.74 \pm 0.06$	$0.13 \pm 0.01$	0.320/3	$0.82 \pm 0.08$	$-(0.02 \pm 0.01)$	0.442/3
$K^+$	$0.023 \pm 0.005$	$0.42 \pm 0.04$	3.436/3	$0.026 \pm 0.006$	$0.22 \pm 0.04$	3.700/3
$K^-$	$0.028 \pm 0.008$	$0.37 \pm 0.05$	11.024/3	$0.03 \pm 0.01$	$0.18 \pm 0.05$	12.514/3
$P$	$0.06 \pm 0.01$	$0.17 \pm 0.04$	4.492/3	$0.06 \pm 0.01$	$0.03 \pm 0.01$	4.054/3
$\bar{P}$	$0.006 \pm 0.002$	$0.24 \pm 0.06$	4.616/3	$0.007 \pm 0.002$	$0.07 \pm 0.04$	4.313/3
$D$	$0.0015 \pm 0.0004$	$0.05 \pm 0.02$	0.635/3	$0.0017 \pm 0.0004$	$-(0.11 \pm 0.04)$	0.656/3

TABLE VI: Values of  $a$ ,  $b$ ,  $\alpha$  and  $\beta$  for production of various secondaries in  $Au + Au$  collisions at  $\sqrt{s_{NN}} = 130$  GeV[ndf=No. of data - No. of parameters in the fit].

Identified	$a$	$\alpha$	$\chi^2/ndf$	$b$	$\beta$	$\chi^2/ndf$
Secondary						
$\pi^+$	$1.6 \pm 0.1$	$0.0015 \pm 0.0003$	0.250/3	$1.6 \pm 0.1$	$-(0.13 \pm 0.01)$	0.221/3
$\pi^-$	$1.3 \pm 0.1$	$0.02 \pm 0.01$	0.190/3	$1.32 \pm 0.07$	$-(0.12 \pm 0.01)$	0.125/3
$K^+$	$0.11 \pm 0.01$	$0.15 \pm 0.01$	0.073/3	$0.12 \pm 0.01$	$-(0.012 \pm 0.002)$	0.083/3
$K^-$	$0.11 \pm 0.03$	$0.11 \pm 0.06$	1.175/3	$0.11 \pm 0.03$	$-(0.03 \pm 0.01)$	1.081/3
$P$	$0.09 \pm 0.01$	$0.10 \pm 0.02$	0.191/3	$0.09 \pm 0.01$	$-(0.05 \pm 0.01)$	0.151/3
$\bar{P}$	$0.06 \pm 0.01$	$0.10 \pm 0.02$	0.148/3	$0.06 \pm 0.01$	$-(0.04 \pm 0.01)$	0.115/3

TABLE VII: Values of  $a$ ,  $b$ ,  $\alpha$  and  $\beta$  for production of various secondaries in  $Au + Au$  collisions at  $\sqrt{s_{NN}} = 200$  GeV[ndf=No. of data - No. of parameters in the fit].

Identified	$a$	$\alpha$	$\chi^2/ndf$	$b$	$\beta$	$\chi^2/ndf$
Secondary						
$\pi^+$	$1.7 \pm 0.1$	$-(0.008 \pm 0.004)$	4.455/8	$1.6 \pm 0.1$	$-(0.12 \pm 0.01)$	0.769/8
$\pi^-$	$1.4 \pm 0.1$	$0.03 \pm 0.01$	1.071/8	$1.5 \pm 0.1$	$-(0.12 \pm 0.01)$	1.015/8
$K^+$	$0.130 \pm 0.004$	$0.13 \pm 0.01$	0.583/8	$0.14 \pm 0.01$	$-(0.03 \pm 0.01)$	0.591/8
$K^-$	$0.12 \pm 0.01$	$0.14 \pm 0.01$	1.657/8	$0.13 \pm 0.01$	$-(0.02 \pm 0.01)$	1.490/8
$P$	$0.063 \pm 0.002$	$0.09 \pm 0.01$	0.264/8	$0.069 \pm 0.003$	$-(0.07 \pm 0.01)$	0.274/8
$\bar{P}$	$0.048 \pm 0.002$	$0.08 \pm 0.01$	0.290/8	$0.053 \pm 0.002$	$-(0.07 \pm 0.01)$	0.347/8

TABLE VIII: Values of  $\langle N_{n-part} \rangle$  and  $\langle N_{q-part} \rangle$  used in Fig.6(a) to normalize  $\frac{dN_{ch}}{d\eta}$ -data for various nucleus-nucleus collisions

Collision type	$\sqrt{s_{NN}}$ (GeV)	Centrality	$\langle N_{n-part} \rangle$	$\langle N_{q-part} \rangle$
<i>Au + Au</i>	AGS	0 – 5%	343[14]	786
<i>Pb + Pb</i>	8.7	0 – 5%	349[15]	856
<i>Pb + Pb</i>	17.2	0 – 5%	362[15]	856
<i>Au + Au</i>	56	0 – 6%	330[16]	823
<i>Au + Au</i>	130	0 – 6%	343[16]	871
<i>Au + Au</i>	200	0 – 6%	344[13]	871

TABLE IX: Values of  $N_{q-part}$  for proton-antiproton collisions at three different c.m. energies as a function of relative probability

Relative Probability	53 GeV	200 GeV	1800 GeV
0-5%	3.2	3.5	4.0
5-10%	2.8	3.1	3.7
10-20%	2.5	2.8	3.3
20-30%	2.1	2.3	2.7
30-40%	1.9	2.0	2.5
40-60%	1.4	1.5	1.7
60-100%	0.9	0.9	1.0

TABLE X: Values of  $\langle N_{q-part} \rangle$  for most central(0 – 5%)  $P + \bar{P}$  collisions at different c.m. energies

$\sqrt{s_{NN}}$ (GeV)	53	200	540	630	900	1800
$\langle N_{q-part} \rangle$	3.2	3.5	3.6	3.7	3.8	4.0

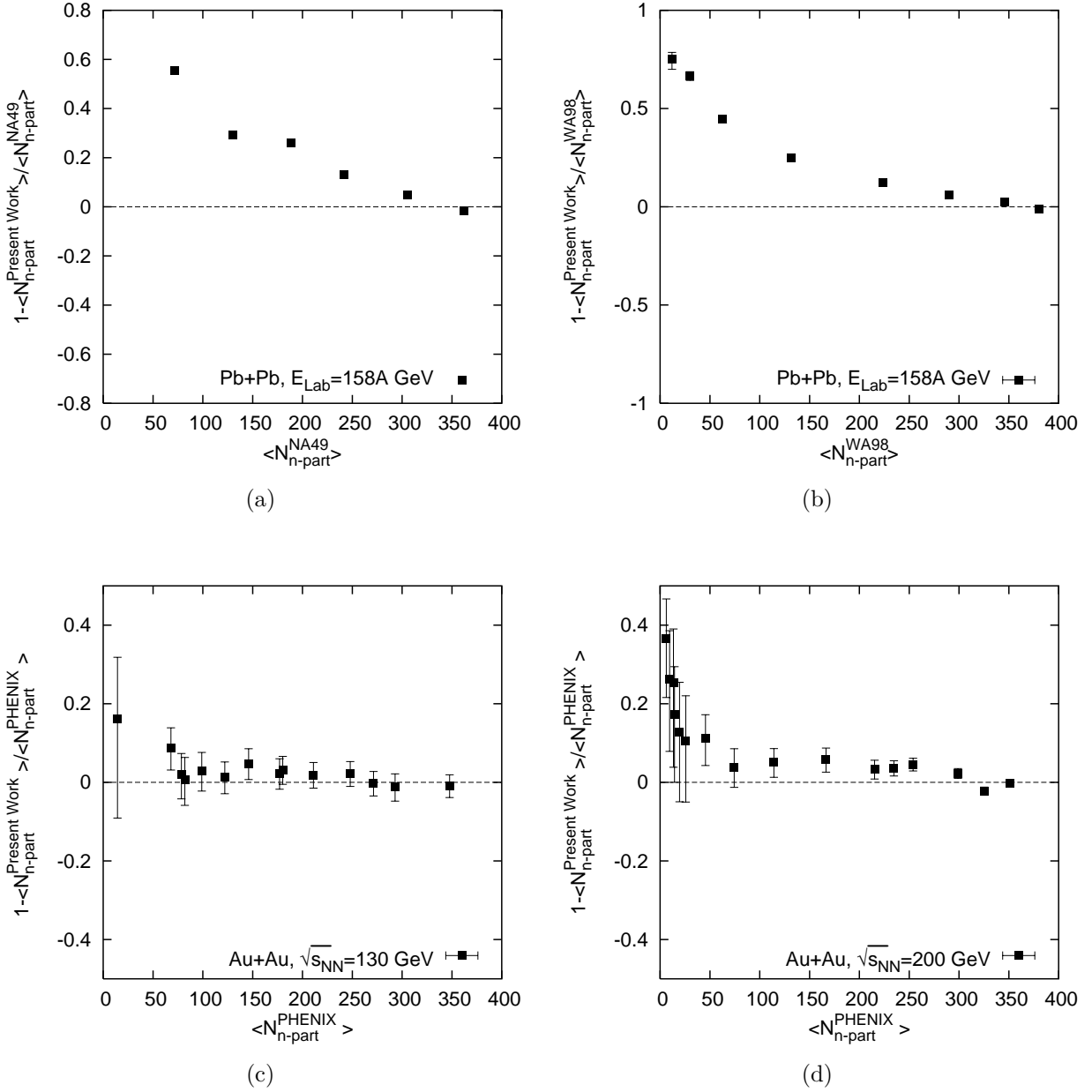
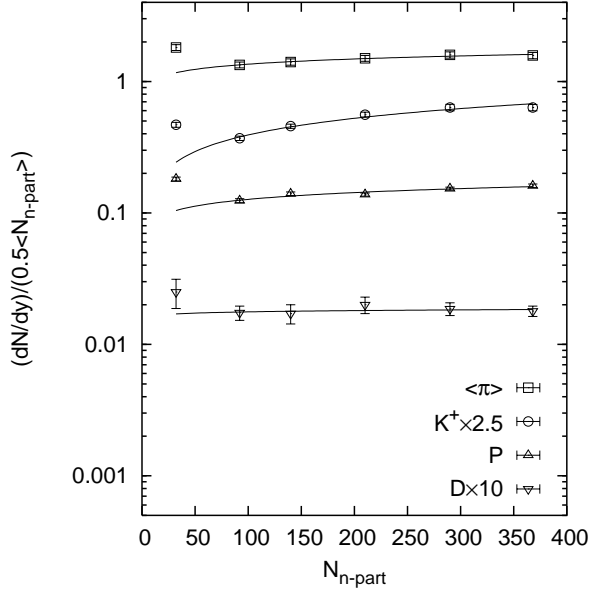
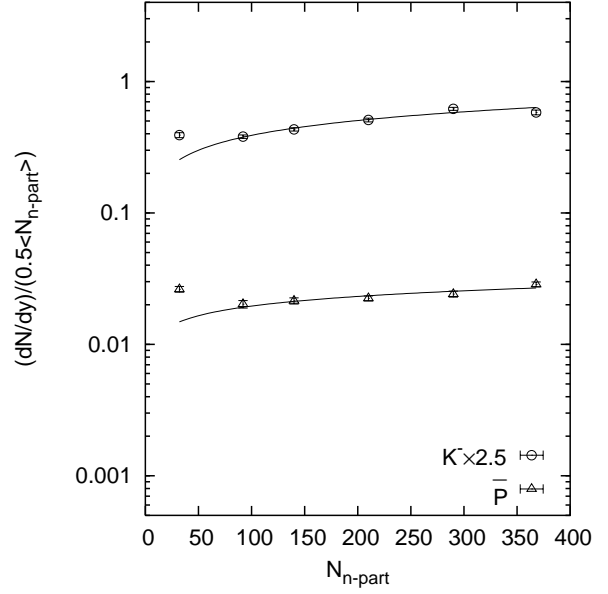


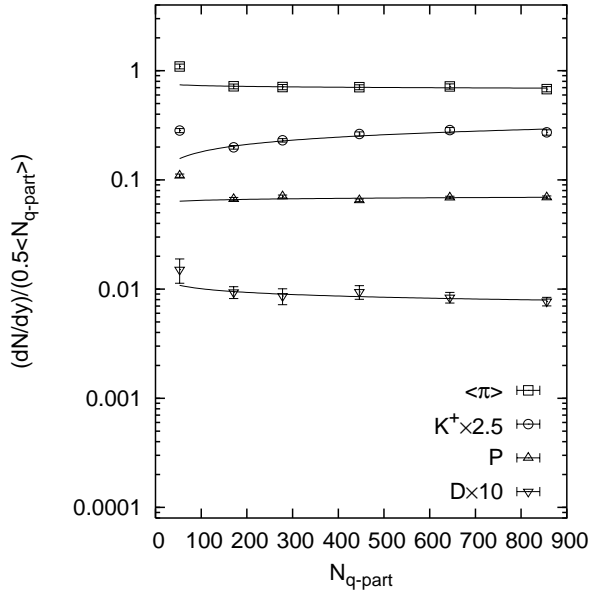
FIG. 2: Comparison of average number of participant nucleons obtained in the present work and by different experimental collaborations in various heavy ion collisions. The experimental data are taken from Ref.[8, 9, 10, 11, 12].



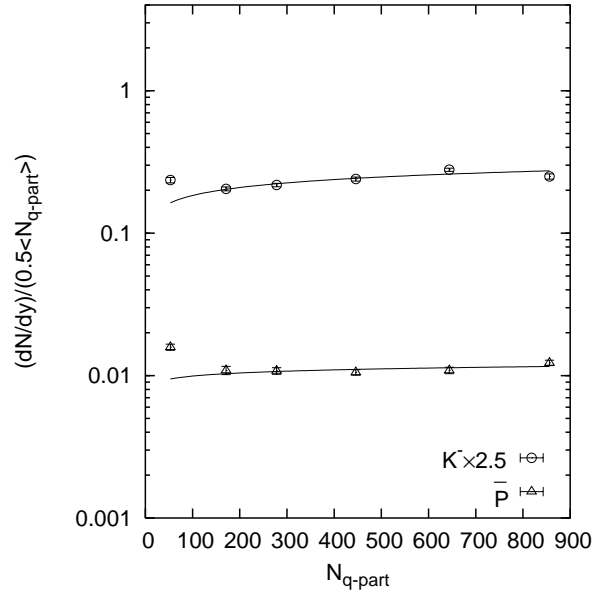
(a)



(b)



(c)



(d)

FIG. 3: Plots of integrated yields normalized by half of the number of participant-nucleons[(a),(b)] or constituent partons[(c),(d)] as a function of centralities for production of the various identified secondaries in  $Pb + Pb$  collisions at  $E_{Lab} = 158A$  GeV[8, 17]. The solid curves represent the fits obtained on the basis of eqn.(5)[(a),(b)] and eqn.(6)[(c),(d)].



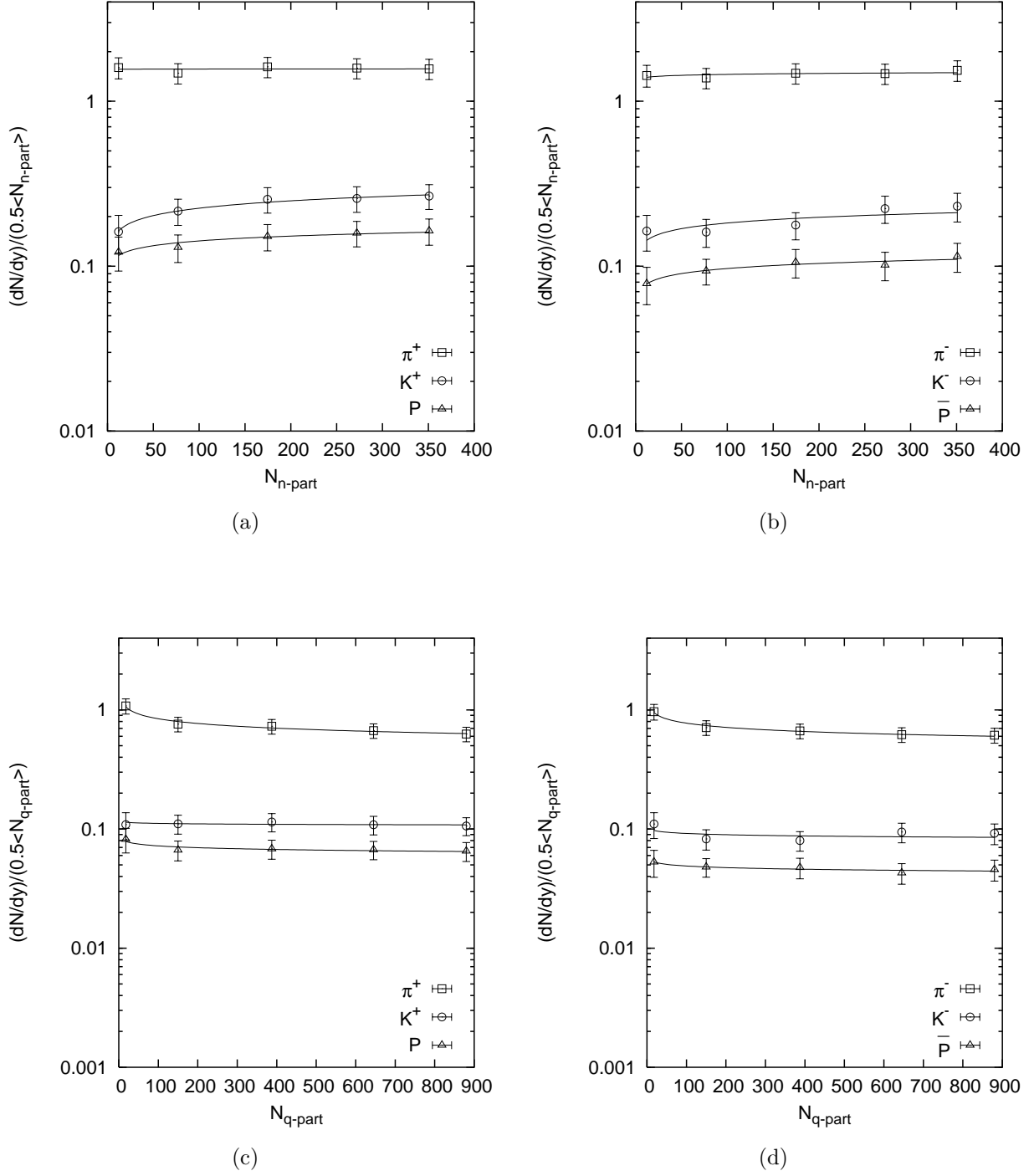


FIG. 4: Plots of integrated yields normalized by half of the number of participant-nucleons[(a),(b)] or constituent partons[(c),(d)] as a function of centralities for production of the various identified secondaries in  $Au + Au$  collisions at  $\sqrt{s_{NN}} = 130$  GeV[10]. The solid curves represent the fits obtained on the basis of eqn.(5)[(a),(b)] and eqn.(6)[(c),(d)].

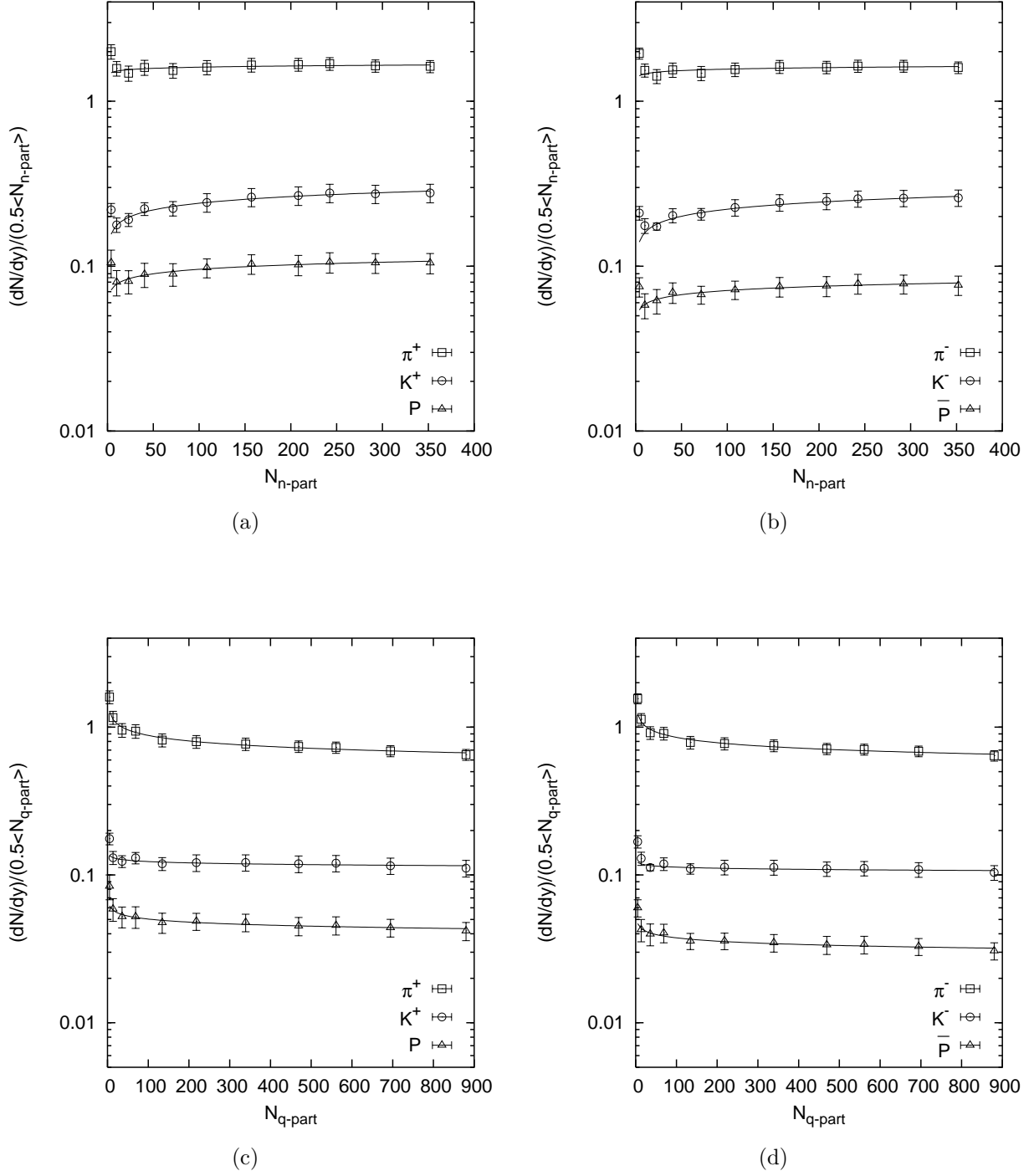
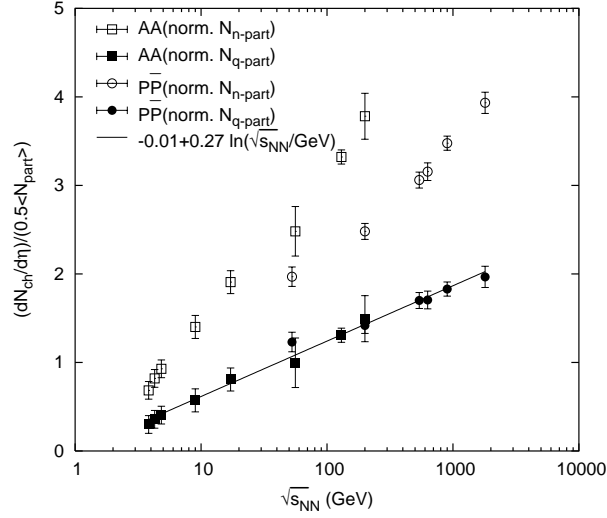
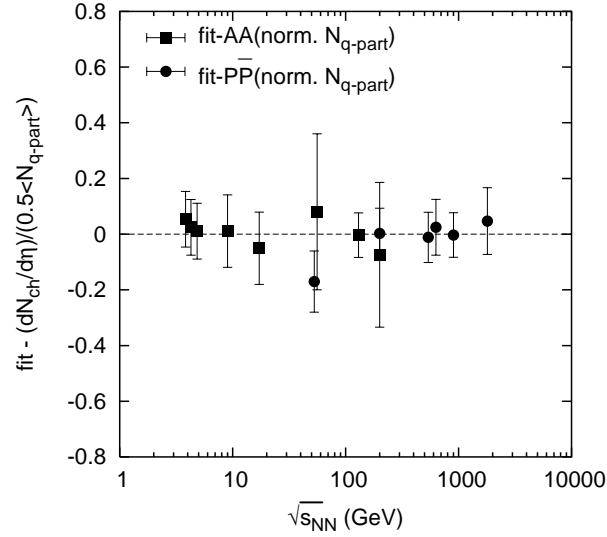


FIG. 5: Plots of integrated yields normalized by half of the number of participant-nucleons[(a),(b)] or constituent partons[(c),(d)] as a function of centralities for production of the various identified secondaries in  $Au + Au$  collisions at  $\sqrt{s_{NN}} = 200$  GeV[12]. The solid curves represent the fits obtained on the basis of eqn.(5)[(a),(b)] and eqn.(6)[(c),(d)].



(a)



(b)

FIG. 6: (a) Energy dependences of integrated yields for charged hadrons produced in different nucleus-nucleus( $A + A$ ) collisions at AGS, SPS and RHIC energies and for the same produced in  $P + \bar{P}$  collisions at ISR energies(Fig.3 of Ref.[13]). The open boxes and open circles provide the data when normalized by half of the average number of participant nucleons for nucleus-nucleus and  $P\bar{P}$  collisions respectively. The solid boxes and solid circles show the same result for  $A + A$  and  $P + \bar{P}$  collisions when normalized by half of the number of the participant-partons. The solid line provide a fit[eqn.(7)] for the nucleus-nucleus and proton-antiproton data when normalized by the half of the corresponding average number of constituent partons. (b) The plot of closeness of the different sets of data with respect to the aforesaid fit.